

The Combined Experimental and Theoretical study of New NLO material N-Acetyl-L-Glutamine

C. Deepa¹, M. Anbuechhiyan^{2*}, Rajendran Sribalan³

¹Department of Physics, Sri Sairam Institute of Technology, West Tambaram,
Chennai-44, India
deepa.phy@sairamit.edu.in

²Department of Physics, SRM Valliammai Engineering College, SRM Nagar,
Kattankulathur– 603203, India
chezhiyan70@gmail.com

³Biochemie Innovations Lab, Tindivanam-604 001, Tamil Nadu, India

Abstract:

N-Acetyl-L-Glutamine (NALG) crystal was grown by slow evaporation solution growth technique. Single crystal X-ray diffraction experiments confirmed the cell parameters. The crystals were subjected to FT-IR and FT-Raman spectral analysis to confirm the functional group of the compound. Thermal stability of the compound was investigated by using thermo gravimetric and differential thermal analysis. The optical study such as photoluminescence emission and UV-Vis transmission spectrum were recorded. Computational studies including molecular geometry optimization, Mulliken atomic charge analysis and HOMO-LUMO analysis were also conducted using the theory level B3LYP method at 6-311+G(d,p) to explore different intermolecular interactions particularly hydrogen bonding. Molecular electrostatic potential is used for visualisation and prediction of possible nucleophilic and electrophilic interactions. The electric dipole moment and first order hyperpolarizability were calculated. The second order NLO studies for N-acetyl-L-Glutamine crystal were done by Kurtz-Perry technique, and it was compared with KDP.

Keywords: NALG crystal; DFT; first order hyperpolarizability; Second Harmonic Generation.

1. Introduction

Non linear optical crystals with high conversion efficiencies for second harmonic generations are desirable, in various key functions such as frequency shifting, optical modulation, optical switching in telecommunications and signal processing [1]. Among these organic materials are of great importance. In π conjugated organic ionic species, the cation is the main source of non linear properties, whereas anion stabilizes the crystal structure through columbic interactions [2, 3].

In organic molecules the amino acid attract particular interest, as it consist of both donor (NH) and acceptor group (C=O) and forms a donor- π -acceptor group. L-Glutamine is an amino acid, present in large amount in the human body. It keeps the required amount of nitrogen within the body and provides proper growth and development of muscles [4]. N-acetyl-L-glutamine is a pharmaceutical drug and is derivate from acetylated-L-Glutamine. It has valuable biological and medical properties, among which one can note is antiulcer agent. These compound also posse's luminescence and non linear properties, which can be applied in optoelectronics.

Researchers have shown interest on the biological and medical application of NALG, only papers with few studies are available to discuss the structure of NALG at molecular level. The first attempt has been made to study the structure of NALG in wide manner by using DFT techniques and also the second harmonic generation efficiency of the material both experimentally and theoretically.

2. Experimental Details

2.1 Materials

The N-acetyl-l-glutamine with analytical grade was purchased from Sigma Aldrich (purity $\geq 98\%$) was used for crystal growth. The main material selection factor depends not only on the laser conditions, but also on the crystal's physical properties [5].

2.2 Synthesis

The saturated solution of NALG was prepared, after several recrystallization processes with various polar solvents. The clear solution was prepared from 10 ml of water in 2g of sample with continuous stirring at room temperature for 30 minutes. The purity of the prepared solution was established by filtration using Whatman-Grade 1 filter paper. The solution is allowed for slower evaporation process. Transparent colourless single crystal of N-acetyl-l-glutamine was grown with optical quality after 3 weeks. The photograph of the crystal is shown in Fig 1.

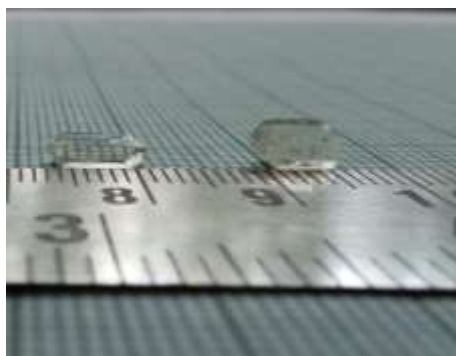


Fig.1. Photograph of the NALG crystal

2.3 Chemical Characterization of NALG crystal

ENRAF NONIUS CAD4 single crystal X-ray diffractometer instrument furnished with Mo $K\alpha$ radiation source of X-rays ($\lambda = 0.7107 \text{ \AA}$) monochromated with graphite monochromator has been engaged to determine unit cell dimensions and space group of NALG grown a single crystal. The powder X-ray diffraction (PXRD) was performed using PANalytical XPERT-PRO instrument for powder crystalline sample of NALG carrying with Cu $K\alpha$ radiation of X-ray source having a wavelength (λ) of 1.5418 \AA in the angle range from 5° to 60° with a scanning resolution of $0.03^\circ/\text{s}$. FTIR and FT-Raman study was done using JASCO FT/IR-410 spectrometer and BRUKER RFS27 spectrometer respectively. The vibration measurements were performed in the frequency range from $4000\text{-}500 \text{ cm}^{-1}$. Shimadzu UV2450 spectrophotometer equipped with photomultiplier tube detector was employed for recording UV-Vis-NIR optical transmittance spectrum in the wavelength region from 200 to 1100 nm. The simultaneous thermo gravimetric (TG) and differential thermal analysis (DTA) were carried out using NETZSCH STA 409 °C thermal analyzer at a heating rate of $20 \text{ }^\circ\text{C}/\text{min}$. The Nd:YAG laser beam (wavelength (λ) of 1064 nm) radiation equipped, modified Kurtz-Perry powder SHG method was utilized for measuring SHG efficiency of powder crystalline sample of NALG single crystal. B3LYP method at 6-311G (d,p) basis level of theory. The optimized geometry, Molecular electrostatic potential, Mulliken atomic charge distribution of the material has been analyzed. The HOMO-LUMO energies were calculated and the band gap has been found.

2.4 Computational Studies of NALG crystal

DFT Computation was performed using Gaussian '09W software package using the computational method has been applied to find the first order hyperpolarizability.

3. Results and Discussions

3.1 Single Crystal XRD analysis

The grown single crystal of NALG has been subjected to Single crystal X-ray diffraction study. The crystal belongs to orthorhombic system with noncentrosymmetric space group $P2_12_12_1$. The unit cell parameters are in good concord with the reported literary value [6], shown in Table 1

Table 1. Lattice parameters value of the grown NALG crystal

| Lattice parameters | Reported | Present work |
|--------------------|-----------------------|---------------------------|
| a | 13.811(10) Å | 13.879 (2) Å |
| b | 5.095(10) Å | 5.013 (3) Å |
| c | 12.914(10) Å | 12.876 (3) Å |
| volume | 908.72 Å ³ | 907.98 (2) Å ³ |
| System | orthorhombic | orthorhombic |
| Space Group | $P2_12_12_1$ | $P2_12_12_1$ |

3.1.1 Powder XRD analysis

The grown single crystal of NALG has been subjected to PXRD. The obtained 2 θ values are used for indexing, by the PROSZKI software package. The sharp peak indicates the good crystallinity of the material which is free from impurity. The experimental powder XRD and the Simulated Powder XRD patterns are revealed in Fig 2. As expected, the intensity variations of experimental patterns are analogous to the simulated patterns.

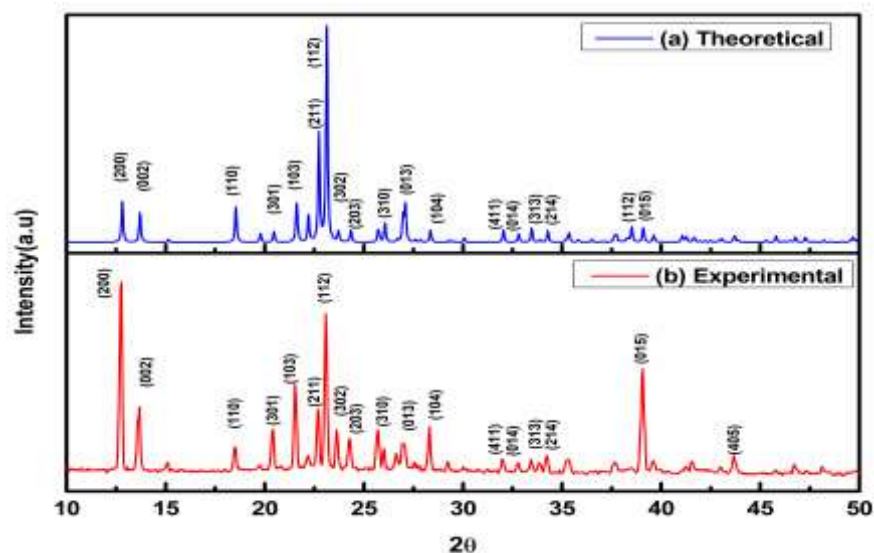


Fig. 2.(a) Experimental and (b) simulated PXRD pattern of NALG.

3.2 Fourier Transform Infrared analysis

The FT-IR spectrum of the grown crystal was shown in Fig.3a. The characteristic absorptions at 3226cm⁻¹ correspond to stretching vibrations ν (O-H).The

absorptions at 3087 cm^{-1} correspond to asymmetric stretching vibrations $\nu(\text{CH}_2)$ [7]. The stretching vibrations $\nu(\text{CH}_2, \text{CH}_3)$ at 2872 cm^{-1} are found. The asymmetric stretching deformation $\nu(\text{CH}_3)$ appeared around 1422 cm^{-1} . The bands at 1382 cm^{-1} are due to $\nu(\text{C-O})$ stretching vibration. The twisting of (CH_2) occurs at band 1253 cm^{-1} . The absorptions at 1177 cm^{-1} corresponds to (C-N) stretching. The rocking of (CH_3) occurs at band 992 cm^{-1} [8]. The (C=O) wagging modes (O-H) torsion occur at band 699 cm^{-1} . The spectral region 606 cm^{-1} are characterized by bands associated to C=O rocking [9]. The observed characteristic FT-IR vibration frequencies are listed in Table 2.

Table 2. FTIR and FT-Raman frequencies with their vibrational assignments of NALG.

| FTIR (cm^{-1}) | Raman (cm^{-1}) | Vibrational assignments |
|---------------------------|----------------------------|--|
| 3445,3348,3226 | 3214 | O-H Stretching |
| 3087 | 3090 | Asymmetric stretching CH_2 |
| 2872 | 2988,2926 | Stretching vibration CH_2, CH_3 |
| 1672 | 1686 | C=O stretching |
| 1422 | 1454 | Asymmetric stretching deformation CH_2, CH_3 |
| 1382,1349 | 1382,1383 | C-O Stretching vibration |
| 1253 | 1293 | Twisting of CH_2 |
| 1177 | 1134 | C-N Stretching |
| 992 | 999 | Rocking of CH_3 |
| 936 | 933 | Hydroxyl out of plane bending |
| 699,648 | 699 | O-H torsion |
| 606,533 | 543 | C=O rocking |

3.2.1 Fourier Transform Raman Analysis

The peak at 3214 cm^{-1} is ascribed to the O-H stretching [10]. The peak at 2988 cm^{-1} is assigned to CH_3 stretching vibration. The intense complex band appears at 2926 cm^{-1} is assigned to asymmetric CH_2 stretching vibration. The band at 1686 cm^{-1} is due to C=O stretching [11]. The peak at 1454 cm^{-1} is given to CH_2 asymmetric deformation. The spectral region 1382 cm^{-1} is characterized by CH_2 deformations. The hydroxyl out of plane bending is attributed to 933 cm^{-1} . The molecule have skeletal bending and torsion vibrations, which give rise to some low wave band less than 500 cm^{-1} . The FTIR-Raman spectrum is shown in Fig 3b.

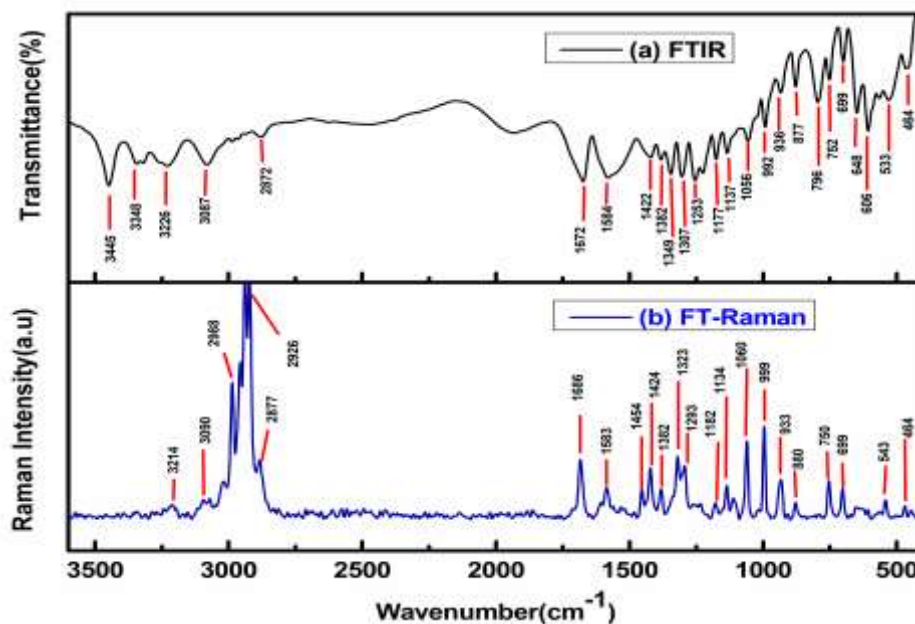


Fig. 3. (a) FTIR and (b) FT-Raman spectrum of NALG crystal

3.3 Thermal studies

Differential and thermo gravimetric analysis was done and TG/DTA curves are shown in Fig 4, From TGA curve NALG crystal is thermally stable up to 198°C. The major weight loss occurs in the temperature range of 198°C -240°C. In major decomposition temperature of the various volatile products like NH₂, CO, CH₂ and a mixture of hydrocarbon gases were liberated. This is complementary with the DTA curve, where there is sharp endothermic peak at 208°C, due to melting point of the compound, where there is a weight loss [12].

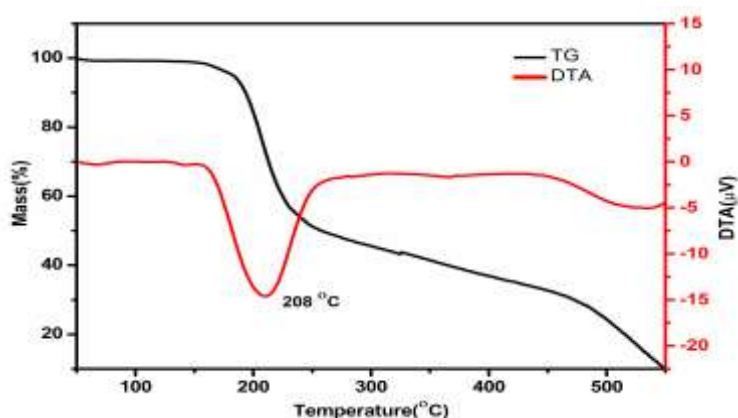


Fig.4. TG /DTA thermo grams of NALG crystal

3.4 Optical analysis

UV-visible-near infrared transmission spectrum was recorded and is shown in Fig 5. The crystal shows good optical transparency in the entire visible region of 400-800nm, with a lower cut off wavelength of 260nm. The 80% transparency in the visible region, with no absorption makes it a good candidate for optoelectronic devices. The presence of maximum absorption at 260 nm is due to $n-\pi^*$ electronic transitions [13]. This transition involves least amount of energy than all the transitions and therefore, this transition gives rise to an absorption band at longer wavelength.

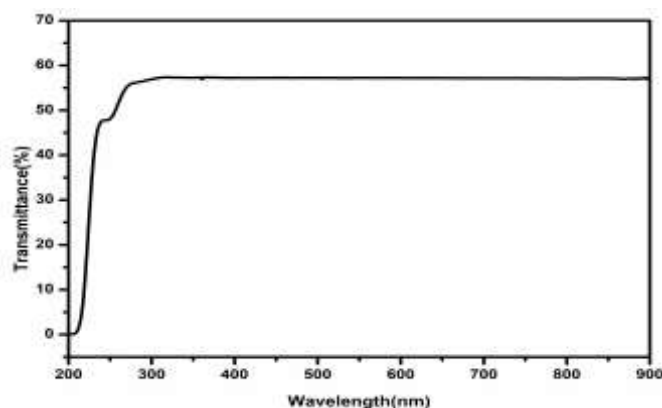


Fig. 5. Optical transmittance spectrum of NALG crystal.

3.5 Photoluminescence studies

The photoluminescence intensity strongly depends on the structural perfection of the crystal. The photoluminescence spectrum of NALG is shown in Fig 6. The compound NALG displays the green emission in the molecule at 545nm. The lower cut off wavelength appears at 530nm, is observed in the spectrum, endorsing the suitability of NALG in optical application [14].

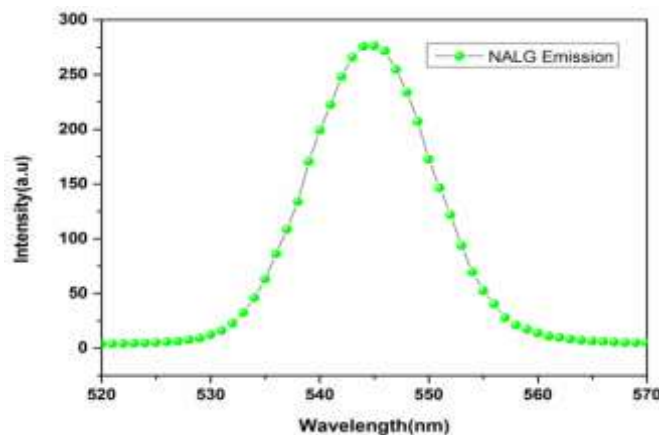


Fig. 6. Photoluminescence spectrum of NALG crystal.

3.6 Second Harmonic Generation

The most widely technique for confirming SHG of the material is Kurtz powder technique. The second harmonic generation has various applications in Fibre optic communications which is interesting among Electrical Engineers. Harmonic efficiency is directly related to the power per unit area of the laser beam [15]. The NALG crystal has non centrosymmetric space group, which is essential condition for SHG. When a Q-Switched Nd-YAG laser of fundamental wavelength 1064 nm was sent through the powdered sample, the wavelength was halved to 532nm, confirming its SHG efficiency [16, 17].The SHG property of NALG crystal was compared with standard KDP crystal. The SHG efficiency of grown crystal is 3.2 times greater than KDP, shown in Fig 7.

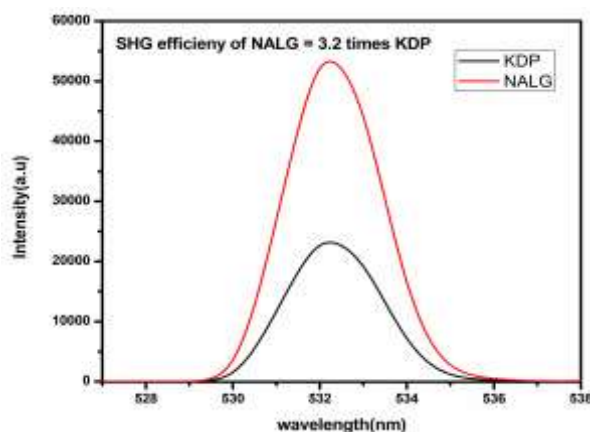


Fig. 7.SHG conversion efficiency comparison between NALG and KDP.

3.7 Optimized Geometry

The structure of NALG crystal was optimized by the B3LYP method at 6.3119+G (d,p) level of theory and structure is shown in Fig 8a & 8b. The single crystal X-ray CIF (Crystallographic Information File) has been given as input. The Optimized parameters have been compared with experimental geometrical parameters and the differences seem too small, which is shown in Table 3. Observed bond length within the side chain is in general agreement, with those reported for L-glutamine [18]. The bond length C5-C6 is 1.513Å is shorter than the expected. The angle (C3-C5-C6) is 111.65° smaller than the usual found in other amino acids and peptides [19-21]. There is non planarity in C3, N1, C2, O1, C1 and NH1, and the best planarity is found in C1, C2, O1, and N1. The non planarity could be due to intermolecular interaction involving hydrogen attached to the peptide nitrogen. The nitrogen of the amide group is slightly pyramidal in character [22] due to hydrogen bonding. The hydrogen atom bonded to C1 are almost staggered with respect to the bond C1=O1. The structure is stabilized by intermolecular hydrogen bonding such as N-H...O and O-H...O. The hydrogen bond distance N1-O4 is shorter than other hydrogen bond distance N2 and oxygen atom.

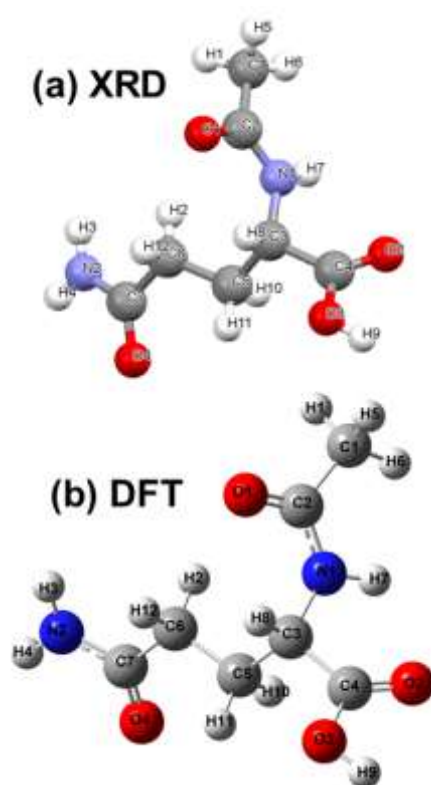


Fig. 8. (a) XRD crystal structure of NALG and (b) DFT optimized structure of NALG.

Table 3. Bond length, bond angles and Torsional angle comparison between XRD and DFT optimized structure of NALG

Bond lengths (Å)

| Parameters | XRD | CC-pVTZ |
|------------|--------|---------|
| C2-N1 | 1.323 | 1.364 |
| C2-O1 | 1.248 | 1.22 |
| C3-C4 | 1.53 | 1.519 |
| C3-C5 | 1.534 | 1.543 |
| C3-N1 | 1.4514 | 1.451 |
| C4-O2 | 1.2035 | 1.205 |
| C4-O3 | 1.303 | 1.345 |
| C5-C6 | 1.512 | 1.523 |
| C6-C7 | 1.513 | 1.523 |
| C7-N2 | 1.33 | 1.362 |
| C7-O4 | 1.2249 | 1.217 |

Bond angles (°)

| Parameters | XRD | CC-pVTZ |
|------------|--------|---------|
| C1-C2-N1 | 116.8 | 115.51 |
| C1-C2-O1 | 121.62 | 121.9 |
| N1-C2-O1 | 121.54 | 122.59 |
| C4-C3-C5 | 110.09 | 109.67 |
| C4-C3-N1 | 111.42 | 108.05 |
| C5-C3-N1 | 111.43 | 113.66 |
| C3-C4-O2 | 124.51 | 124.92 |
| C3-C4-O3 | 110.98 | 111.92 |
| O2-C4-O3 | 124.5 | 123.14 |
| C3-C5-C6 | 111.65 | 112.55 |
| C5-C6-C7 | 113.57 | 112.25 |
| C6-C7-N2 | 114.97 | 114.52 |
| C6-C7-O4 | 122.04 | 123.32 |
| N2-C7-O4 | 122.97 | 122.15 |
| C2-N1-C3 | 120.94 | 122.16 |

Torsion angles (°)

| Parameters | XRD | CC-pVTZ |
|-------------|---------|---------|
| C1-C2-N1-C3 | -171.76 | 171.24 |
| O1-C2-N1-C3 | 5.85 | -9.48 |
| C5-C3-C4-O2 | 105.68 | 109.56 |
| C5-C3-C4-O3 | -73.21 | -69.11 |
| N1-C3-C4-O2 | -18.47 | -14.83 |
| N1-C3-C4-O3 | 162.64 | 166.51 |
| C4-C3-C5-C6 | 178.93 | 175.94 |
| N1-C3-C5-C6 | -56.92 | -63.01 |
| C4-C3-N1-C2 | -134.78 | -135.52 |
| C5-C3-N1-C2 | 101.82 | 102.53 |
| C3-C5-C6-C7 | -176.49 | 178.86 |
| C5-C6-C7-N2 | -154.35 | 169.69 |
| C5-C6-C7-O4 | 26.84 | -10.97 |
| C1-C2-N1-C3 | -171.76 | 171.24 |
| O1-C2-N1-C3 | 5.85 | -9.48 |

3.8 Mulliken Population Analysis

The Mulliken population analysis delivers the distribution of electrons in a molecule and derives at atomic charge effect, dipole moment, molecular polarizability and more a lot of properties of molecular systems [23]. The atomic charge values of O3, nitrogen (N1,N2) and carbon (C1,C5,C6) have a negative charge and behaved as electron donors. The remaining atoms except H10 have

positive charge, behaved as acceptors, which is shown in Fig 9a. The hydrogen atom H9 (0.220) poses higher value than other hydrogen atom due to involvement in intermolecular hydrogen bonding interaction. The N1 is less negative than N2, which connects the amide and acetyl group. The atomic charge values are shown in Table4.

Table 4. Mulliken atomic charge distribution analysis of NALG molecule.

| Atom | Charge | Atom | Charge |
|------|--------|------|--------|
| C1 | -0.294 | H1 | 0.114 |
| C2 | 0.229 | H2 | 0.118 |
| C3 | 0.011 | H3 | 0.162 |
| C4 | 0.285 | H4 | 0.157 |
| C5 | -0.151 | H5 | 0.119 |
| C6 | -0.222 | H6 | 0.087 |
| C7 | 0.238 | H7 | 0.147 |
| N1 | -0.165 | H8 | 0.124 |
| N2 | -0.235 | H9 | 0.22 |
| H12 | 0.11 | H10 | -0.151 |
| | | H11 | 0.112 |

3.9 Electrostatic Potential Analysis

The Molecular Electrostatic Potential (MEP) is a useful tool to investigate the molecular structure [24, 25]. The electrostatic potential is produced by the electrons and the nuclei of the molecule, which is used for visualization and prediction of electrophilic and nucleophilic region[26]. The molecular electrostatic potential is given in increasing colour code red>white>blue, indicating negative, neutral and positive respectively [27]. From the MESP map Fig 9b of NALG, it is clear that the carbonyl (C=O) lies in the most electronegative region (red), which is suitable for electrophilic attack and the NH2 group lies in the electropositive region (blue), which is suitable for nucleophilic attack.

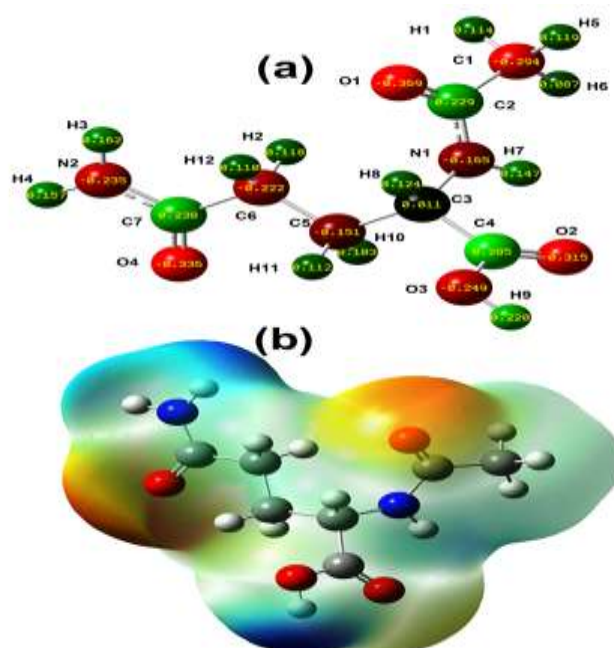


Fig. 9. (a) Mulliken atomic charge distribution and (b) Molecular electrostatic potential (MEP)

4. Frontier Molecular Orbital Analysis

The molecules are categorized by a separation of highest occupied molecular orbital (HOMO) and the lowest unoccupied molecular orbital (LUMO). The HOMO is the ability to donate an electron and the LUMO is the ability to accept electron. HOMO-LUMO plays a significant role in chemical reactivity, kinetic stability, optical polarizability and the hardness (or softness) of a molecular system [28, 29]. If $E_{\text{lumo}} - E_{\text{homo}}$ shows less value, then the material has high reactivity, softer and more polarisable. The HOMO-LUMO energy is calculated by B3LYP method at 6.3119+G (d, p) basis set. The HOMO-LUMO energy values are -7.04eV and -0.41eV respectively, and the energy gap is 6.64 eV, which is shown in Fig 10. NALG molecule, which is considered, exhibited lower values than those of urea (7.364eV) and KDP (8.364eV).

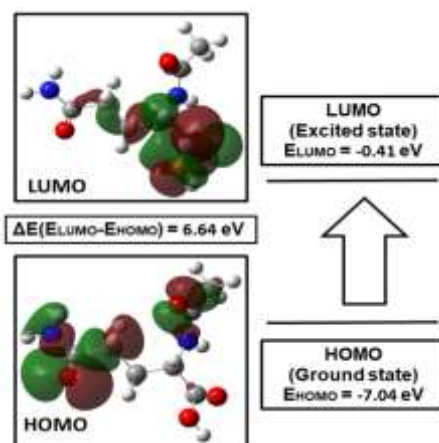


Fig. 10. HOMO and LUMO orbital of NALG molecule.

4.1 First Order Polarizability

NALG molecule is having non-zero dipole moment and hyperpolarizabilities. In order to have high molecular hyperpolarizability, the organic molecules should possess a good number of π electrons and extend delocalization[30]. The polarizability(α) and hyperpolarizability(β) of NALG crystal are calculated using B3LYP method using at 6.3119+G (d,p) basis set. The calculated mean polarizability (α) value of NALG is $107.85 \cdot 10^{-24}$ and the first order hyperpolarizability (β) is $801.5 \cdot 10^{-33} \text{ e.s.u.}$ The highest contributing component in NALG is in β_{xyy} direction with $663.98 \cdot 10^{-33} \text{ e.s.u.}$, which is clear evidence of dipole moment. The electric dipole moment for NALG is found to be 1.30 debye. The polarizability (α) and hyperpolarizability (β) and dipole moment values obtained from Gaussian output, are reported in atomic units(a.m.u) given in Table.5.

Table 5. The calculated electric dipole moment (μ_0), mean polarizability (α_0) and first order hyperpolarizability (β_{total}) components of the NALG molecule.

| α (esu x 10 ⁻²⁴) | | β (esu x 10 ⁻³³) | | β_{xzz} | 297.93 |
|-------------------------------------|--------|------------------------------------|---------|----------------------|--------|
| α_{xx} | 17.12 | β_{xxx} | -350.03 | β_{yzz} | 214.11 |
| α_{xy} | -0.12 | β_{xxy} | -39.53 | β_{zzz} | -222.5 |
| α_{yy} | 17.6 | β_{xyy} | 663.98 | β_{total} | 801.55 |
| α_{xz} | -1.12 | β_{yyy} | 303.31 | Dipolemoment (Debye) | |
| α_{yz} | 0.59 | β_{xxz} | -36.98 | μ_x | 0.38 |
| α_{zz} | 13.17 | β_{xyx} | 95.28 | μ_y | 1.18 |
| α_0 | 107.85 | β_{yyz} | 274.5 | μ_z | 0.38 |
| | | | | μ | 1.3 |

5. Conclusion

An organic material NALG was synthesized and the single crystals were grown by slow evaporation method at room temperature, which is optically transparent, colourless and NLO active. The grown crystal crystallizes in orthorhombic system with the space group of P2₁2₁2₁. The various functional groups were identified using FTIR and FT-Raman spectroscopy. The UV-vis transmission spectroscopy shows that the crystal has transparency in the visible region (400-800nm) which is need for SHG. Thermo grams showed that the material is steady up to 198°C, is suitable for device fabrication. Second harmonic generation efficiency of the crystal is found to be 3.2 times greater than KDP, which makes the material suitable candidate for NLO application. The quantum chemical calculation such as optimized geometry, Mulliken charge analysis, is used to discuss various molecular interactions. MEP study indicates that, positive electrostatic potential for the NH⁺ group of cation and negative electrostatic potential around carbonyl group. Homo-Lumo energy groups were evaluated and found to be 6.64 eV. The calculated first order hyperpolarizability (β) of NALG crystal is 801.5*10⁻³³e.s.u, which indicates the usefulness of NALG in optical applications.

References

- [1] Pal, T. Kar, T., Bocelli, G., & Rigi, L. "Synthesis, Growth, and Characterization of l-Arginine Acetate Crystal: A Potential NLO Material", *Crystal Growth & Design*, 3(1), (2003), 13–16.
- [2] X. Liu, Z. Yang, D. Wang and H. Cao, "Molecular Structures and second order nonlinear optical Properties of ionic organic crystal materials", *Crystals* 6(2016), 158-177.
- [3] L. Chandra, J. Chandrasekeran, K. Perumal, B. Babu, "Third order nonlinear optical and Electrical properties of new 2-aminopyridinium 2-chloro 4-nitrobenzoate single crystals", *Optik* 127(2016) 3206-3210.

- [4] Sheela, G. E., Manimaran, D., Joe, I. H., Jothy, V. B. "Studies on Molecular Structure and Vibrational Spectra of NLO Crystal L-Glutamine Oxalate by DFT Method", *Indian Journal of Science and Technology*, 10(31),(2017), 1–23.
- [5] M. Anbuhezhiyan, S. Ponnusamy, C. Muthamizhchelvan, "Synthesis, characterization and nonlinear optical studies of L-Leucinium Oxalate: a single crystal", *Optoelectronics and Advanced Materials – Rapid Communications* Vol. 3, No. 11, November 2009, p. 1161 – 1167.
- [6] M.R.Narasimhamurthy, K.Venkatesan, F.Winkler, "Crystal and molecular structure of N-acetyl-L-glutamine", *J.Chem.Soc. Perkin Trans.2*,(1976) 768.
- [7] Kausar, N., Alexander, B. D., Dines, T. J., Withnall, R., & Chowdhry, B. Z. "Vibrational spectroscopy and DFT calculations of amino acid derivatives: N-acetyl-L-Asp and N-acetyl-L- Glu in the solid state", *Journal of Raman Spectroscopy*, 40(6), (2009) 670–678.
- [8] P.Dhamelincourt, F.J.Ramirez," Vibrational spectra and assignments of amino acid L-asparagine", *J.RamanSpectrosc.* (1991), 22, 577.
- [9] G.Socrates, *Infrared Characteristic Frequencies*, 1980.Wiley-Interscience, Chichester.
- [10] J.T.L.Navarrette, V.Hernandez, F.J.Ramirez, *J. Mol. Struct.* (1995), 348,249.
- [11] J.T.Edsall, *J.Chem.Phys.* (1937), 5, 50.
- [12] Sathya, K., Dhamodharan, P., & Dhandapani, M. "Hydrogen bonded 2-methyl-1H-imidazol-3-ium 3,5-dinitrobenzoate 3,5-dinitrobenzoic acid, a new optical crystal: Evaluation of properties by structural, spectral, quantum chemical calculations, Z-scan and Hirshfeld studies", *Journal of Physics and Chemistry of Solids*, 114, (2018), 228–239.
- [13] S. Jin , J. Zhang , D. Wang, L. Tao , M. Zhou, Y. Shen, Q. Chena, Z. Lin, X. Gao, *J. Mol. Struc.* 1065 (2014) 223-234.
- [14] Hanumantharao, R., & Kalainathan, S. *Studies on structural, thermal and optical properties of novel NLO crystal bis L-glutamine sodium nitrate. Materials Letters*, 74,(2012), 74–77.
- [15] T.Shanmugavadivu, M.Dhandapani, "Crystal Structure, spectral, thermal, optical laser damage, NLO study and quantum chemical calculations of a non-centrosymmetric crystal N, N- diphenylguanidinium p-toluenesulphonate, *Journal of Molecular Structure*, Vol 1179,5 March (2019),pg 651-661.
- [16] S.K. Kurtz, T.t. Perry, a powder technique for the evaluation of nonlinear optical Materials. *J. Appl. Phys.* 39(1968) 3798-3813.
- [17] H.O. Marcy, M.J. Tosker, L.F. Warren, C.H. Cunningham, C.A.Thomas, "L.Histidine tetrafluoroborate: a solution grown 'Semiorganic", crystal for non linear frequency Conversion, *Opt. Lett.* 209(1995) 252-254.
- [18] T. F. Koltzle, M. N. Frey, M. S. Lehmann, and W. C. Hamilton, *Acta Cryst.*, (1973), B29, 2571
- [19] Y. C. Leung and R. E. Marsh, *Acta Cryst.* (1958), 11, 17.
- [20] D. A. Wright and R. E. Marsh, *Acta Cryst.* (1962), 15, 54.
- [21] P. S. Naganathan and K. Venkatesan, *Acta Cryst.* (1971), B27, 1079
- [22] F. Winkler and J. D. Dunitz, *J. Mol. Biol.*, (1971), 59, 169.
- [23] Usha, C., Santhakumari, R., Joseph, L., Sajan, D., Meenakshi, R., & Sinthiya, A. "Growth and combined experimental and quantum chemical study of glycyl-L-Valine crystal", *Heliyon*, 5(5),(2019), e01574.

- [24] Murray J SandSenK, **1996**, *Molecular Electrostatic Potentials .Concepts and Applications* (Amsterdam: Elsevier)
- [25] SeminarioJ, M. **1996**, *Recent Development and Applications of Modern Density Functional Theory* (Amsterdam: Elsevier)
- [26] VERMA,P.,Srivastava, A., Shukla, A.,Tandon,, & Shimpi, M.R. “Vibrational spectra, hydrogen bonding interactions and chemical reactivity analysis of nicotinamide-citric acid co crystal by an experimental and theoretical approach”, (**2019**), *New Journal of Chemistry*.
- [27] E. Scrocco, J. Tomasi, *Electronic molecular structure, reactivity and intermolecular forces: a euristic interpretation by means of electronic molecular potentials. Adv. Quant. Chem. 11 (1978) 115-193.*
- [28] M.Ucak-Astarlioglu, S.Edwards and C. A.Zoto, *J.Lab.Chem. Educ.*, 5, 32–39. (**2017**),64[29].S. Radhakrishnan, R. Parthasarathi, V. Subramanian and N. Somanathan, *Comput. Mater. Sci.*, (**2006**), 37, 318–322.
- [29] S.Sivaraman, A. Agilandeswari, C. Balakrishnan, R.M.Sockalingam,S.P. Meenakshisundaram, R. Markkandan, “Supramolecular architecture and computational Studies of nicotinodrazide and furan-2- carbohydrazide”, *Journal of Molecular Structure, Volume 1173, 5 Dec 2018, pages 385-397.*